Electronic Supplementary Materials

For https://doi.org/10.1631/jzus.A2500365

Impact of urban heat island and global warming on multi-energy complementarity optimization of buildings: application to typical office buildings in Hangzhou, China

Qingqing MIAO[1,2,3], Xiaoyu LUO[1,2,3], Jiang LU[4], Weijun GAO[5], Yucong XUE[6], Yifan FAN[1,2,3], Jian GE[1,3], Jiahong ZHAO[1,2,3]

[1]*College of Civil Engineering and Architecture, Zhejiang University, Hangzhou 310058, China*
[2]*Center of Balance Architecture, Zhejiang University, Hangzhou 310028, China*
[3]*Architectural Design and Research Institute Co. Ltd., Zhejiang University, Hangzhou 310028, China*
[4]*School of Civil Engineering and Architecture, Zhejiang University of Science and Technology, Hangzhou 310023, China*
[5]*Faculty of Environmental Engineering, The University of Kitakyushu, Kitakyushu 8080135, Japan*
[6]*China United Engineering Co. Ltd., Hangzhou 310056, China*

Table S1 Detailed information about GCMs

GCM	Research institutes	Country	Resolution (latitude×longitude grid points)
ACCESS-ESM1-5	CSIRO	Australia	145×192
BCC-CSM2-MR	BCC	China	160×320
CESM2-WACCM	NCAR	America	192×288
CESM2	NCAR	America	192×288
GFDL-ESM4	GFDL	America	180×288
CanESM5	CCCma	Canada	64×128
CMCC-CM2-SR5	CMCC	Italy	192×288
MPI-ESM1-2-LR	MPI-M	Germany	96×192
MIROC6	MIROC	Japan	128×256
MRI-ESM2-0	MRI	Japan	160×320
INM-CM5-0	INM	Russia	120×180
IPSL-CM6A-LR	IPSL	France	143×144

Table S2 UWG input parameters

Input parameters	Value	Unit
Meteorological and site parameters (Salvati and Kolokotroni, 2023)		
Location	Hangzhou	-
Longitude	120.21	°
Latitude	30.24	°
Urban Boundary Layer Height - Day	1000	m
Urban Boundary Layer Height - Night	50	m
Inversion Height	150	m
RSM Temperature Reference Height	2	m
RSM Wind Reference Height	10	m

Circulation Coefficient	1.2	-
UCM-UBL Exchange Coefficient	1	-
Day Threshold (for UBL night/day)	50	W/m^2
Night Threshold (for UBL night/day)	50	W/m^2
Minimum wind velocity	0.1	m/s
Rural Average Obstacle Height	0.1	m
Urban characteristics		
Average Building Height	60	m
Fraction of waste heat into canyon	1	-
Building Density	0.2	-
Vertical to Horizontal Ratio	1.09	-
Urban Area Characteristic Length	305	m
Max Dx	50	m
Road Albedo	0.15	-
Pavement Thickness	0.5	m
Sensible Anthropogenic Heat (Peak)	25	W/m^2
Latent Anthropogenic Heat (Peak)	2.5	W/m^2
Vegetation variables		
Urban Area Veg Coverage	0.35	-
Urban Area Tree Coverage	0.04	-
Veg Start Month	1	-
Veg End Month	12	-
Vegetation Albedo	0.25	-
Latent Fraction of Grass	0.5	-
Latent Fraction of Tree	0.5	-
Rural Road Vegetation Coverage	0.8	-
Building characteristics (Ministry of Housing and Urban-Rural Development of China, 2015)		
R-value	1.67	m^2·K/W
R-value	1.82	m^2·K/W
U-Factor	1.50	W/m^2·K
SHGC	0.35	-
Coefficient of Performance	3.5	-
Lighting load density	9	W/m^2
Equipment load density	15	W/m^2
Occupancy density	10	m^2/person
ACH	0.3	-

Table S3 Parameter settings for a typical large office building

Parameter	value
Location	Hangzhou
Geometry parameters	Building area: 43331m^2; Floors: 20
Envelope U-value (W/m^2·K)	Wall: 0.6; Roof: 0.55; Window: 1.5
Fresh air (m^3/h·person)	30
Personnel density (m^2/person)	10
Lighting power density (W/m^2)	9
Equipment power (W/m^2)	15
HVAC COP	Cooling: 3.5; Heating: 3

Table S4 Taylor skill score (TSS) Ranking

GCM	Combined	Shanghai	Changsha	Hangzhou	Zhumadian	Chengdu
ACCESS-ESM1-5	9	12	3	9	4	1
BCC-CSM2-MR	11	11	9	6	10	8
CESM2-WACCM	3	4	4	4	7	5
CESM2	4	2	6	5	8	6
GFDL-ESM4	1	7	1	3	1	3
CanESM5	10	6	12	11	11	11
CMCC-CM2-SR5	2	3	2	2	2	4
MPI-ESM1-2-LR	8	10	5	8	6	2
MIROC6	5	5	7	10	5	9
MRI-ESM2-0	7	1	8	7	9	10
INM-CM5-0	6	9	11	1	3	7
IPSL-CM6A-LR	12	8	10	12	12	12

Table S5 Configuration parameters of building energy system for different climate scenarios

Scenario			Initial invest-ment (10^6 CNY)	PV (kW)	MG (kW)	Battery (kW)	Grid purchase (MWh)	Export to the grid (MWh)	Peak energy consumption (kWh)
TMY			7.08	250	600	1209	2253.83	64.78	1831.21
2040s	SSP 245	FC	7.64	250	650	1361	2267.22	62.69	1910.15
		FUM	7.59	250	650	1207	2272.37	62.31	1858.95
	SSP 585	FC	7.66	250	650	1379	2278.35	65.06	1927.81
		FUM	7.61	250	650	1279	2285.97	64.03	1870.97
2080s	SSP 245	FC	8.12	250	700	1317	2269.83	69.32	1938.57
		FUM	7.67	250	650	1427	2305.57	70.18	1913.34
	SSP 585	FC	8.62	250	750	1303	2316.80	68.02	1950.91
		FUM	8.12	250	700	1325	2321.16	70.81	1911.68

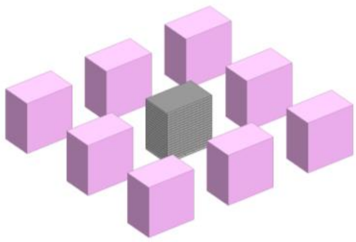

Fig. S1 Typical Building Model

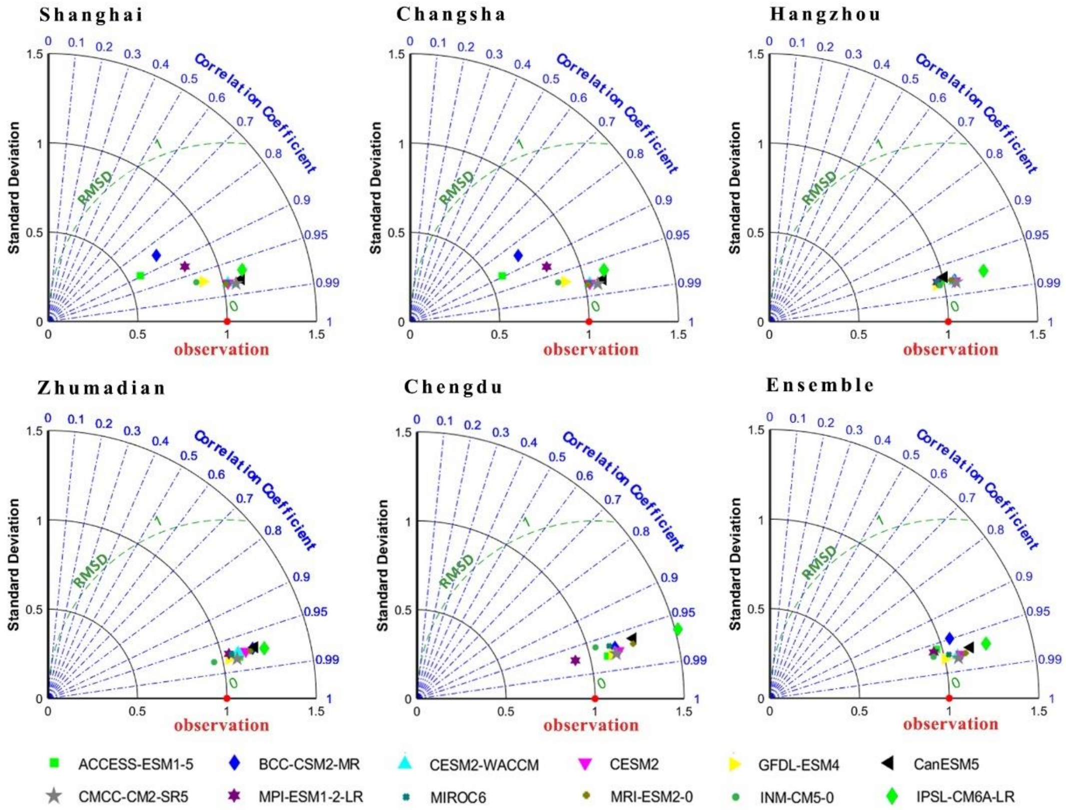

Fig. S2 Air temperature applicability evaluation

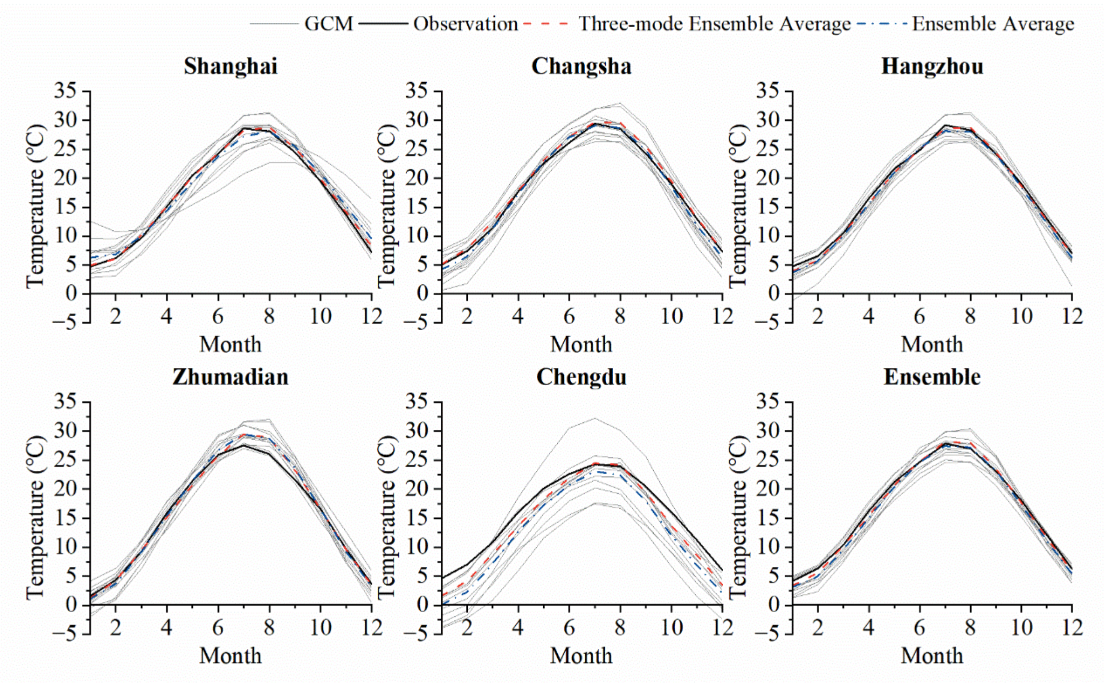

Fig. S3 Comparison of individual GCM, all GCM ensembles, and preferred GCM ensembles with site observations

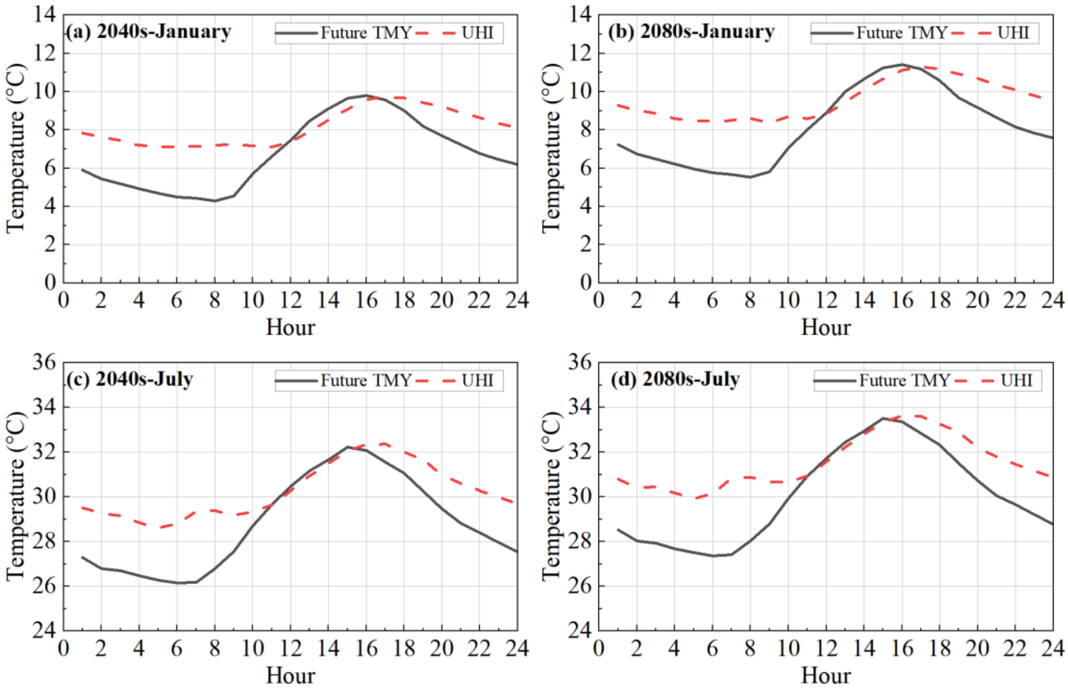

Fig. S4 Mean air temperature changes under SSP245: (a) January in the 2040s, (b) January in the 2080s, (c) July in the 2040s, (d) July in the 2080s (The black solid line shows a future TMY and the red dashed line shows the influence of the future urban temperature considering UHI effect.

Section S1

1) Shift: A change is applied to the baseline data to reflect the absolute value changes caused by climate change. This approach is suitable for meteorological parameters without specific upper or lower limits, such as atmospheric pressure. The formula is as Eq. (S1).

$$x = x_0 + \Delta x_m \tag{S1}$$

where x is the future hourly climatic variable; x_0 is the historical hourly climatic variable; Δx_m is the absolute change in the monthly mean value of the variable for the month m.

2) Stretch: The baseline data is scaled proportionally to represent relative changes. This method is suitable for parameters with clearly defined upper and lower limits, such as solar radiation, wind speed, and precipitation. The formula is as Eq. (S2).

$$x = \alpha_m x_0 \tag{S2}$$

where α_m is the fractional change in the monthly-mean value for month m.

3) A combination of shift and stretch: This method simulates situations with both absolute and relative changes. It is suitable for temperature parameters where both mean values and amplitude changes need to be considered during the morphing process. The formula is as Eq. (S3).

$$x = x_0 + \Delta x_m + \alpha_m (x_0 - \langle x_0 \rangle_m) \tag{S3}$$

where $\langle x_0 \rangle_m$ is the monthly mean values of existing variable for the month m.

Section S2

Relevant economic parameters are set as shown in Table S6 (Tian, 2021), where O&M costs is the operation and maintenance costs, and pollutant emission factors and treatment costs are shown in Table S7 (Li et al., 2021). The price for the purchase and sale of electricity are shown in Table S8 (State Grid Zhejiang Electric Power Company Limited, 2024), where the electricity selling price is set at 70% of the Electricity purchase price (Li, 2020). Additional assumptions include (Zhang, 2023): a 7.5 m² footprint per 1 kW of PV panels, a maximum PV capacity of 250 kW due to roof constraints; the energy stored in the batteries is quantified by the state of charge (SOC), and in order to prolong the life of the batteries to avoid excessive discharging, the SOC of the batteries used is limited to 20%~100%; no allowable unmet load, and a system lifetime of 20 years.

Table S6 Economic parameters of building energy system components

Parameter	PV	Battery	Converter	MG
Initial investment costs (CNY/kW)	2500	300	300	10000
Replacement costs (CNY/kW)	2500	300	300	8000
O&M costs (CNY/year)	10	10	0	0.02
Life time (year)	25	5	20	45000 h

Table S7 Pollutant emission factors and treatment costs

Pollutant type	Treatment costs (CNY/kg)	Pollutant emission factors (g/kWh)		
		PV	MG	Grid
CO_2	0.023	0	742	542
SO_2	6	0	0.0036	2.74
NO_x	8	0	0.2	1.34

Table S8 Time-of-use price for grid

Time-of-use	Electricity purchase price (CNY/kWh)	Electricity selling price (CNY/kWh)
Sharp	1.2277	0.8594
Peak	0.8440	0.5908
Shoulder	0.6975	0.4883
Off-peak	0.3627	0.2539

Section S3

1) PV system

Solar energy is an important renewable energy source, in PV system, the output power of PV panel is affected by solar radiation, operating temperature and other factors. The output power of PV panels is calculated using the Eq. (S4) (Fathima and Palanisamy, 2015).

$$P_{PV} = Y_{PV} f_{PV} \left(\frac{\overline{G}_T}{\overline{G}_{T,STC}}\right) \left[1 + \alpha_P \left(T_c - T_{c,STC}\right)\right] \quad (S4)$$

where Y_{PV} is the rated capacity of the PV array, meaning its power output under standard test conditions (kW). f_{PV} is the PV derating factor (%). $\overline{G}_T$ is the solar radiation incident on the PV array in the current time step (kW/m^2). $\overline{G}_{T,STC}$ is the incident radiation at standard test conditions (1 kW/m^2). α_P is the temperature coefficient of power (%/°C). T_c is the PV cell temperature in the current time step (°C). $T_{c,STC}$ is the PV cell temperature under standard test conditions (25 °C).

2) MG

Gas turbines are characterized by high efficiency, long life, small size and low pollution, which traditional diesel generators do not have. They generate electricity by consuming fuel, with the output power adjustable in real time through fuel supply, allowing for a fast response. The operating efficiency of a gas turbine is calculated as Eq. (S5) (Li, et al., 2021).

$$\eta_{MT}(t) = 0.0753\left[\frac{P_{MT}(t)}{65}\right]^3 - 0.3095\left[\frac{P_{MT}(t)}{65}\right]^2 + 0.4174\frac{P_{MT}(t)}{65} + 0.1068 \quad (S5)$$

where $P_{MT}(t)$ is the active output power of the MG.

3) Battery

Since the output of renewable energy is affected by environmental factors and has significant instability and uncertainty, the energy storage battery can effectively regulate the power fluctuation of the system and improve the system stability. The SOC of the battery is calculated as Eq. (S6) (Li, et al., 2021).

$$SOC(t) = \begin{cases} SOC(t-1) + \frac{1}{\eta^-}P_{bess}(t), P_{bess}(t) \le 0 \\ SOC(t-1) + \eta^+ P_{bess}(t), P_{bess}(t) > 0 \end{cases} \quad (S6)$$

where $P_{bess}(t)$ is the charging and discharging power of the battery at the moment t. Positive means charging and negative means discharging. η^+ and η^- are the charging and discharging efficiency respectively.

Section S4

1) Power balance constraint

$$P_{PV}(t) + P_{MT}(t) + P_{grid}(t) + P_{bess}(t) = P_L(t) \quad (S7)$$

where $P_{PV}(t)$, $P_{MT}(t)$, $P_{grid}(t)$, and $P_{bess}(t)$ are the output power of the PV, MG, grid and battery at moment t, respectively. $P_L(t)$ is the electrical load demand at moment t.

2) MG constraint

$$\begin{cases} P_{MT}^{min}(t) \le P_{MT}(t) \le P_{MT}^{max}(t) \\ |P_{MT}(t) - P_{MT}(t-1)| \le r_{MT} \end{cases} \quad (S8)$$

where $P_{MT}^{min}(t)$ and $P_{MT}^{max}(t)$ are the upper and lower bounds of the output power of the MG. r_{MT} is the upper limit of the ramping rate of the MG.

3) Battery constraint

$$\begin{cases} P_{bess}^{min}(t) \le P_{bess}(t) \le P_{bess}^{max}(t) \\ SOC^{min}(t) \le SOC(t) \le SOC^{max}(t) \end{cases} \quad (S9)$$

where $P_{bess}^{min}(t)$ and $P_{bess}^{max}(t)$ are the upper and lower bounds of the output power of the storage battery unit. $SOC^{min}(t)$ and $SOC^{max}(t)$ are the upper and lower limits of the energy storage capacity, respectively.

4) Grid constraint

$$P_{grid}^{min}(t) \le P_{grid}(t) \le P_{grid}^{max}(t) \quad (S10)$$

where $P_{grid}^{min}(t)$ and $P_{grid}^{max}(t)$ are the upper and lower limits of the power of the linking-up road, respectively. The upper limit is set to 50% of the peak load following previous literature (Perera et al., 2017).

Section S5

Fig. S5 shows the percentage change in cooling, heating, and overall energy demand for a typical office building in Hangzhou under the FC and FUM relative to the energy demand under TMY. Cooling demand for office building tends to increase under all future paths and increases further with increasing paths. In the 2040s, cooling demand increases by 32.5%, 28.9%, 34.4%, and 38.6% under the four paths, respectively. In the 2080s, with rising temperature, cooling demand further increases compared to the 2040s. The driving effect of climate warming on cooling demand continues to strengthen over the long term. Heating demand shows a decreasing trend, primarily due to the rise in winter temperature, which reduces the heating load. As a result, in the 2040s, heating demand decreases by 18.5% to 24.3% across the four paths, and in the 2080s, it decreases by 31.6% to 44%. The FUM further amplifies the impact of FC on cooling and heating demands. Compared to FC scenarios, cooling demand increases by an additional 0.83% to 5.84%, while heating demand decreases by an additional 13.1% to 15.4%. After offsetting the impacts of increased cooling demand and reduced heating demand, the overall building energy demand still shows a consistent upward trend. This is because cooling dominates in Hangzhou, with cooling energy consumption accounting for a larger share of total building energy consumption compared to heating. Under the FC, overall energy demand increases by 3.9% to 15%, while under the FUM, it increases by 4.2% to 14.4%.

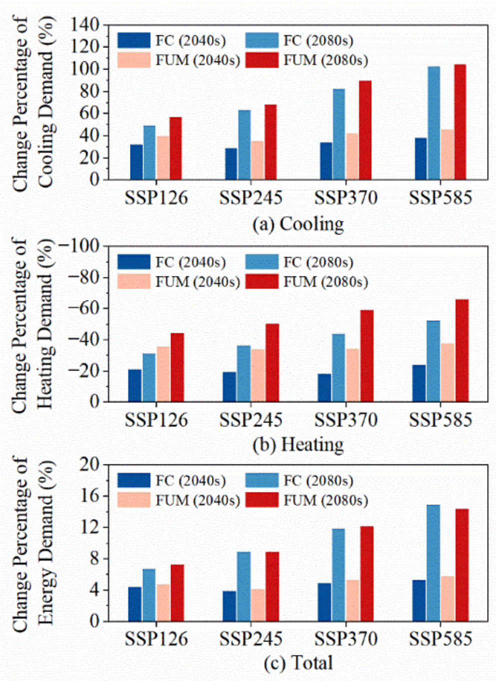

Fig. S5 Percentage change in (a) cooling, (b) heating and (c) overall energy demand relative to TMY